

Green synthesis of silver oxide nanoparticles and its antibacterial activity against dental pathogens

Velu Manikandan^{1,2} · Palanivel Velmurugan¹ · Jung-Hee Park¹ · Woo-Suk Chang³ · Yool-Jin Park⁴ · Palaniyappan Jayanthi² · Min Cho¹ · Byung-Taek Oh^{1,5}

Received: 18 December 2016 / Accepted: 22 February 2017 / Published online: 27 April 2017
© Springer-Verlag Berlin Heidelberg 2017

Abstract In the present study, the use of silver oxide nanoparticles (Ag₂O NPs) synthesized using *Ficus benghalensis* prop root extract (FBPRE) as a reducing and stabilizing agent is reported and evaluated for its antibacterial activity against dental bacterial strains. The effects of pH, extract concentration, metal ion concentration, and contact time were studied to confirm the optimum production of Ag₂O NPs. Our results suggest that, by increasing the extract concentration and the time frame, there will be a significant increase in the formation of nanoparticles. The UV–vis adsorption spectra show the absorbance peak in the range of 430 nm, and FTIR spectral peaks indicate that the phytochemicals in the extract are responsible for the formation of the nanoparticles. The HR-TEM image, SAED, and XRD pattern confirmed the

morphology (spherical), silver oxide 42.7 nm and silver 51.4 nm, and crystalline nature of the obtained nanoparticles, respectively. The blend of FBPRE and Ag₂O NPs showed excellent antibacterial activities against the two dental bacteria *Streptococcus mutans* and *Lactobacilli* sp. The study results suggest that the blend of synthesized Ag₂O NPs and FBPRE will be useful in tooth paste as a germicidal agent after extensive investigation with animal models.

Keywords Silver oxide · Nanoparticles · *Ficus benghalensis* · Optimization · Characterization · Antibacterial

Introduction

In recent years, research in nanotechnology has flourished using green chemicals for the synthesis of several metallic nanoparticles without the addition of any external chemicals responsible for causing environmental contamination (Amin et al. 2012; Velmurugan et al. 2014; Muthukrishnan et al. 2015). Green route-mediated synthesis of metallic nanoparticles is attained using extracts from various plants and their parts as a reducing and capping agent (Velmurugan et al. 2015; Palanisamy et al. 2017). Among several metallic nanoparticles studied, the noble metal silver holds a prominent place in nanomaterial research due to its unique properties feasible to apply in various fields. The properties are sensing, optoelectronic, catalysis, and drug delivery (Velmurugan et al. 2016; Dong et al. 2017). Fundamental properties of molecular, supra-molecular, and atomic levels of object could be understood by the help of nanotechnology (Velmurugan et al. 2016). However, the production of nanoparticles using the chemical methods

✉ Min Cho
cho317@jbnu.ac.kr

✉ Byung-Taek Oh
btoh@jbnu.ac.kr

¹ Division of Biotechnology, Advanced Institute of Environment and Bioscience, College of Environmental and Bioresource Sciences, Chonbuk National University, Iksan, Jeonbuk 54596, South Korea

² Department of Environmental Science, Periyar University, Salem 636011, Tamil Nadu, India

³ Department of Biology, University of Texas-Arlington, Arlington, TX 76019, USA

⁴ Department of Ecology Landscape Architecture-Design, College of Environmental and Bioresource Sciences, Chonbuk National University, Iksan, Jeonbuk 54596, South Korea

⁵ Plant Medical Research Center, College of Agricultural and Life Sciences, Chonbuk National University, Jeonju, Jeonbuk 54896, South Korea

available is often expensive, uses lethal chemicals, and is time consuming and cost prohibitive. Therefore, there is a need for eco-friendly, quick, inexpensive, and less time-consuming techniques to produce nanoparticles. Several previous studies have addressed the simple synthesis of such materials without focusing on optimizing production. In our study, we employed *Ficus benghalensis* prop root extract to produce silver nanoparticles and optimized the production process.

Ficus benghalensis (FB) (Moraceae) is commonly known as the Banyan tree in Ayurveda treatment. The *Ficus* species contain more than 2000 varieties and 800 species and are native of world tropics (Aswar et al. 2008; Ahmad et al. 2011). This tree is endemic to Bangladesh, India, and Sri Lanka. Extracts of various plant parts of *F. benghalensis* have been known for their anathematic, analgesic, anti-inflammatory, antioxidant, antidiabetic, immuno-modulatory, and antimicrobial activities since ancient times, and the prop root has been used for tooth-aches. The stem, leaf, bark, fruit, and sap extracts of *F. benghalensis* have been used as an ayurvedic medicines to cure various diseases like dysentery, teeth disorders, skin disorders like sores, piles, diarrhea, and rheumatism, and to boost the immune system (Nidhiya et al. 2010; Kumar et al. 2010; Panday and Rauniar 2016).

Streptococcus mutans and *Lactobacilli* sp. change the environment of the oral flora, enabling fastidious organisms to colonize and cause the formation of dental plaques (Marsh 2010). These two bacteria are normally present in low numbers in the plaque of affected individuals. When salivary flow decreases, the pH of the plaque drops, leading to selection of aciduric (acid-tolerant) bacteria such as *S. mutans* and *Lactobacilli* sp. (Marcotte and Lavoie 1998). This sequence of events indicates that *S. mutans* is involved in the initiation of decay, whereas the *Lactobacilli* sp. is associated with the progression of lesions (Loesche 1986; Marsh 2010).

Herein, we evaluated the potential of the green synthesis of noble metal silver nanoparticles and production optimization and characterized their antibacterial activity against the dental bacteria *S. mutans* and *L. acidophilus* using *Ficus benghalensis* prop root extract (FBPRE).

Materials and methods

Chemicals and biological materials

The AgNO_3 (99.9%) reactant was acquired from DaeJung Chemicals, Seoul, South Korea, in stoichiometric amounts and was dissolved in aqueous solution as the metal precursor. Dried *Ficus benghalensis* prop root (Fig. 1) was obtained from the Periyar University Campus, Salem,

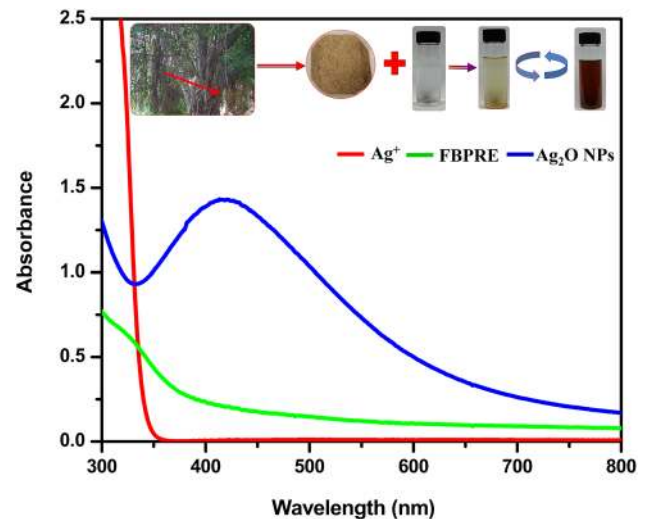


Fig. 1 UV-vis adsorption spectra of Ag_2O NPs, FBPRE, and Ag^+ ; the inset shows the color change in the reaction mixtures of whole tree (*Ficus benghalensis*), prop root, and powder of the *Ficus benghalensis* prop root

Tamil Nadu, India, and the extract was prepared by grinding the dried root into a fine powder. 100 g of this powder was added to 500 mL of deionized water in a 1000-mL flask, mixed well, and maintained on a magnetic heating stirrer at 90 °C for 1 h. The extract yield was filtered for further use. Strains of the dental bacteria *Streptococcus mutans* (KACC 16833) and *Lactobacilli* sp. (KACC 12419) were procured from the Korean Agriculture Culture Collection (KACC) in Suwon, South Korea. Each strain was initially cultivated using nutrient agar, followed by incubation and storage at 4 °C for further use.

Synthesis and optimization of silver oxide nanoparticles

For the synthesis of silver oxide nanoparticles (Ag_2O NPs), FBPRE 10 mL was added to 90 mL of 1 mM silver nitrate solution in 250-mL Erlenmeyer flasks to form a reaction mixture, and the reaction was performed under ambient conditions. Initial confirmation of silver nanoparticle production is by change in color from light yellow to dark brown in the reaction mixture (Fig. 1). The SPR of nanoparticles was measured using a UV-vis spectrophotometer (UV-1800, Shimadzu, Kyoto, Japan) within a working wavelength range of 300–800 nm using a dual beam operated at 1 nm resolution.

Production and optimization of silver oxide *Ficus benghalensis* prop root extract nanoparticles

To optimize the nanoparticle production, parameters such as pH 3.0–10.0; Ag^+ : FBPRE 44.5:0.5–40:5.0 mL; Ag^+ at

0.1–1.0 mM concentrations; and a time frame of 0–270.0 min were tested. Once silver nanoparticle production was complete, the obtained product was centrifuged for 15 min at 12,000 rpm, followed by several washes with copious amounts of nanopure water and ethanol to ensure separation of free entities from the silver nanoparticles. The obtained material was freeze-dried to make a powder and used for further characterization and antibacterial studies.

Characterization

Fourier transform infrared (FTIR) spectra were recorded to detect functional groups involved in nanoparticle synthesis and were obtained using a Perkin–Elmer FTIR spectrophotometer (Norwalk, CT, USA) at a resolution of 4/cm in a diffuse reflectance mode using KBr pellets. High-resolution transmission electron microscopy and selected area electron diffraction (SAED) pattern (HR-TEM model, JEOL-2010, Japan) were used to examine the surface morphology, size, and crystalline structure of the silver nanoparticles. X-ray powder diffraction of the nanoparticles was obtained using a Rigaku X-ray diffraction meter (XRD, Rigaku, Japan) to confirm the crystalline nature of the obtained silver nanoparticles.

Bactericidal activity against dental pathogens

The bactericidal activities were tested by assessing the zone of inhibition (ZoI) and minimum bactericidal concentration (MBC) of the obtained Ag₂O NPs. For culture enrichment, each culture was aseptically inoculated into brain heart infusion (BHI) broth and incubated. Later, the antibacterial sensitivity profile of each strain was tested by spreading 50 µl of each overnight culture grown in BHI on Mueller–Hinton agar (MHA) plates. Each of the MHA plates was prepared with four wells using a sterile juice straw and a control well with penicillin antibiotics (20 µg). Different concentrations of extract powder (50, 100, 150, 200, and 250 µg), Ag₂O NPs, and commercial silver nanoparticles were added to each well on the agar plates loaded with bacterial culture and then incubated at 30 °C for 48 h. After incubation, the plates were examined for clear zone formation. The presence of a clear zone around each well was recorded as inhibition against the bacterial strains. The diameters of such zones were measured using zone measuring scale, and the mean value expressed in millimeters.

To determine the MBC, the obtained extract powder, Ag₂O NPs, and commercial silver nanoparticles were placed in the above described concentrations in test tubes with 3 mL of Luria–Bertani (LB) Broth and 0.1 mL of each bacterial culture and then incubated for 48 h in a

reciprocating shaker. Later, 50 µL of each bacterial culture was spread over the LB agar at a suitable dilution, and the colonies of the viable cells were counted. The antibacterial activity was defined as the percentage of microbe reduction (Lee et al. 2013; Velmurugan et al. 2014, 2015) and was calculated according to AATCC 100, as shown in Eq. (1).

$$R(\%) = \frac{A - B}{A} \times 100, \quad (1)$$

where *A* is total of bacteria obtained from the tubes without Ag₂O NPs after 24 h of incubation and *B* is the number of bacteria according to the “A” conditions with Ag₂O NPs in different concentrations. Consequently, *R* (%) is the percentage reduction ratio, which indicates the biostatic efficiency. Each experiment was performed in triplicate, and the mean ± the standard deviation (SD) are presented as the final values.

Results and discussion

UV–vis analysis

The initial visual confirmation of silver nanoparticle production was performed through visual observation as color change (Fig. 1). Images of the *Ficus benghalensis* whole tree, prop root, powder, and extract and the reaction mixture are shown in (Fig. 1).

The UV–vis spectrum shows a surface plasmon resonance peak (SPR) at 430 nm, which corresponds to AgNP production (Okafor et al. 2013). Our results were in well agreement with earlier findings of Okafor et al. (2013), who studied the in vitro micropropagation of a high-value endangered medicinal plant species, *Phlomis bracteosa*, in order to explore its biogenic potential in biomimetic synthesis of antimicrobial AgNPs. The exact mechanism of the plant extract-mediated synthesis of silver nanoparticles is not well understood nor has it been investigated in depth. It was hypothesized that the bioactive compounds present in the plant extract, such as poly-phenols (flavonoids), have hydroxyl and ketonic groups that bind to the bulk metal silver to reduce it to nano-size.

Production optimization

Figure 2a depicts the formation of silver nanoparticles at different pH. At pH 9, the maximum production of silver nanoparticles was observed, and the spectral peaks at 410 nm and 420 nm for pH 9 and pH 8, respectively. The inset of (Fig. 2a) shows the color change at different pH values from 3 to 10, which indicated that higher amounts of AgNP formation occurred at pH 9. Chitra and Annadurai (2014) stated that the band at 420 nm indicated the

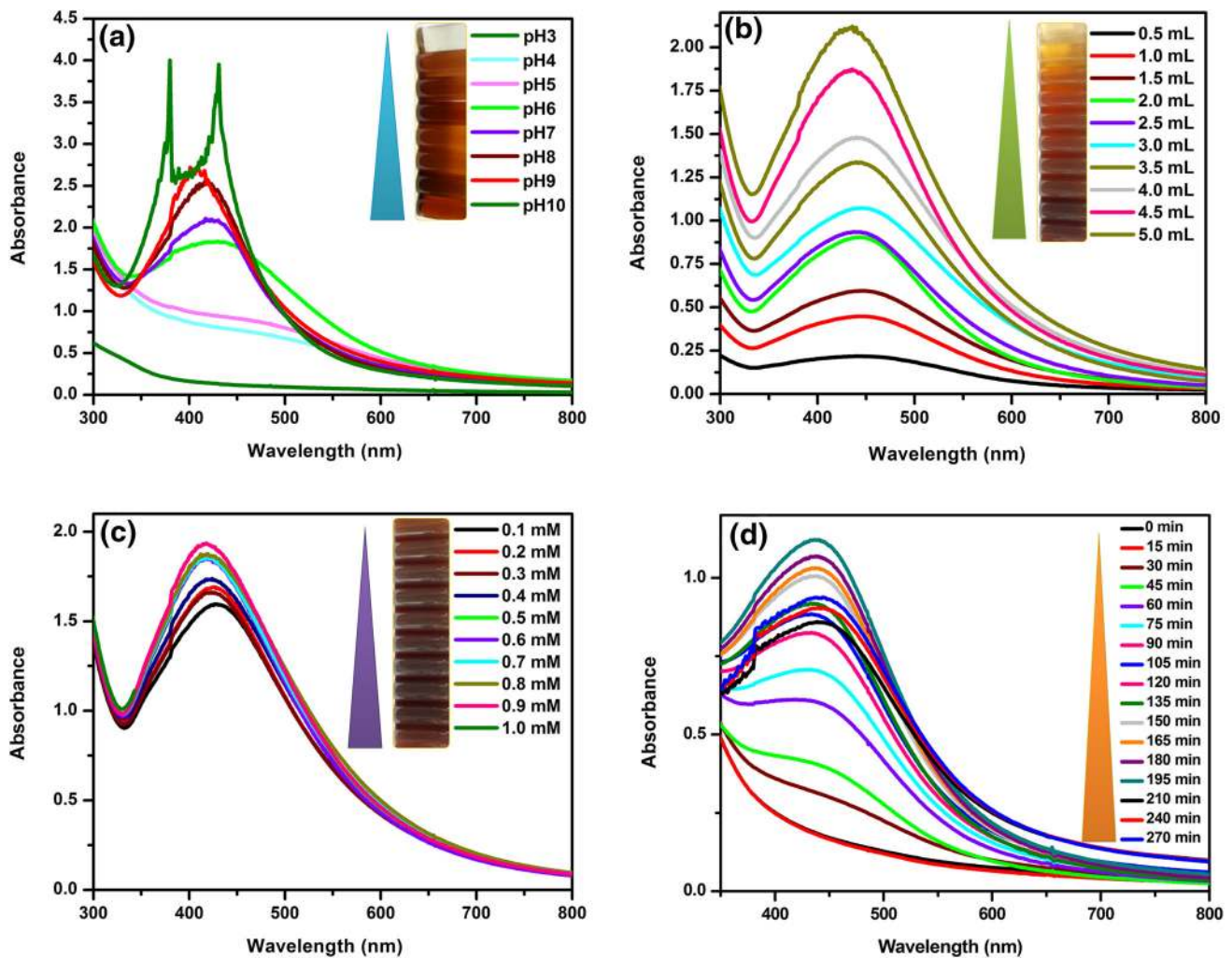


Fig. 2 UV-vis absorption spectra of the optimization of parameters for the production of Ag_2O NPs with different pHs (a), ratios of FBPRE from 0.5 to 5 mL (b), concentration of metal ions Ag^+ from 0.1 to 1.0 mM (c) and different times from 0 to 270 min (d)

spherical shape of the nanoparticles, whereas the particle sizes varied according to the spectral range. The concentration of hydrogen ions plays a key role in nanoparticle formation. In our study, the absorbance band was increased when the pH was increased from 4 to 9 for silver nanoparticle production. A lower and broader absorbance in the silver nanoparticles was observed at lower pH compared to higher pH, which could be due to the larger size of the NPs at a lower pH. It has been demonstrated that pH affects the shape and size of the nanoparticles and also influences the synthetic process used to produce silver nanoparticles (Dwivedi and Gopal 2010; Vanaja et al. 2013; Velmurugan et al. 2015). Our results suggest that an acidic pH suppressing nanoparticle formation is due to increased precipitation or agglomeration, which occurs due to the instability of the nanoparticles (or the lack of a stabilizing agent). Previously, Velmurugan et al. (2014) reported that, at a lower pH, agglomeration occurred due to

over-nucleation and formation of larger size nanoparticles. Conversely, at a high pH, many nanoparticles with smaller surface areas are present due to the bioavailability of functional groups in the *Ficus benghalensis* prop root extract. Figure 2b shows the UV-vis spectra of the synthesized silver nanoparticles with different concentrations of FBPRE (0.5–5 mL) at 1 mM AgNO_3 . With increases in the FBPRE (in 50 mL of 1 mM Ag^+ solution) from 0.5 to 5 mL, the peak absorbance was consistently increased (Fig. 2b). The SPR band appeared with little variation related to the concentration of the extract. The broad SPR at lower quantities of the FBPRE might be the large anisotropic particles formation (Velmurugan et al. 2014). This might have occurred because, in lowering the quantity of FBPRE, the concentration of groups/molecules such as phenolics, alkaloids, and sugars responsible for capping and stabilizing of nanoparticle decreases. These results indicate that higher reduction was achieved at FBPRE

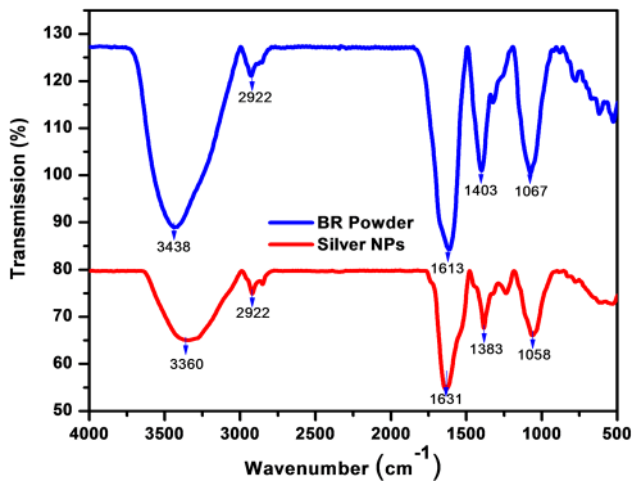


Fig. 3 FTIR spectra of FBPRES and Ag₂O NPs

concentrations of 5 mL (Fig. 2b). These results also corroborate earlier findings with plant extract-based synthesis of silver nanoparticles (Pourmortazavi et al. 2015; Ahmed et al. 2016; Verma and Mehata 2016; Ibrahim 2015), which discussed *Eucalyptus oleosa*, *Azadirachta indica*, and banana peel. Upon evaluating the effects of the different concentrations of silver ions in the reaction mixture, the maximum peak absorbance (using UV-vis) found at 0.9 mM silver ion concentration resulted in good production (Fig. 2c). The SPR peak of the silver nanoparticles became distinct with an increase in the concentration of silver nitrate, and the maximum peak intensity was obtained at 0.9 mM of AgNO₃ (Fig. 2c). Variations in the biological material and metal salt concentration are known to influence nanoparticle synthesis (Verma and Mehata 2016; Ibrahim 2015). This could be caused by an

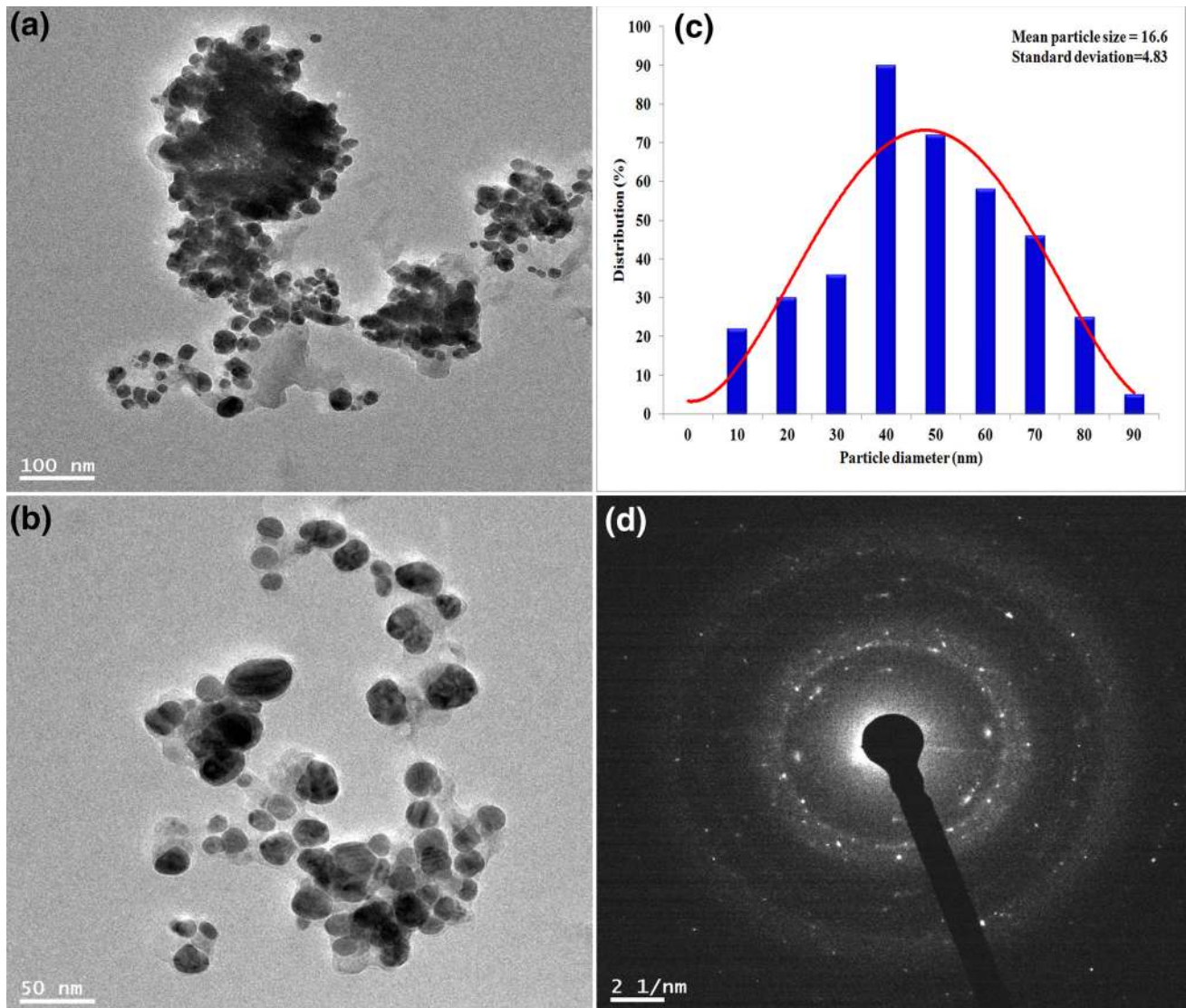


Fig. 4 TEM images of Ag₂O NPs, particle size histogram, and corresponding SAED pattern of Ag₂O NPs

enhancement in the oxidation of hydroxyl groups due to the metal ions (Kora et al. 2010; Shankar et al. 2004). Upon evaluation of the production time frame, higher silver nanoparticle production was observed at 180 min (Fig. 2d). The gradual color change was directly proportional to the incubation time of the reaction mixture increase (Fig. 2d) insert). The rate of reduction of silver ions was slow at 45 min, as an indication of low absorbance values at wavelengths 400–440 nm (Fig. 2d). Our results correlated with the earlier findings of (Shankar et al. 2004; Verma and Mehata 2016). After the longer incubation time, there is no shift in peak wavelength in the SPR band. According to Mie's theory (Shankar et al. 2004; Raut Rajesh et al. 2009), the absorption spectra of spherical AgNPs exhibit a single SPR band, and increasing anisotropy increases the number of peaks.

Characterization of Ag₂O NPS

FTIR

The major functional groups on the FBPRES surface were identified with help of FTIR measurements and their possible involvement in the synthesis of silver nanoparticles. The spectra of FBPRES control and with silver nitrate are presented in (Fig. 3). The control spectrum (FBPRE alone) showed several peaks as an indication of extract is in complex nature. The bands appearing at 3438, 2922, 1613, 1403, and 1067/cm were assigned to the O–H of alcohol stretching vibration or the N–H of amines; C=O of carboxylic acid or ester; N–C=O amide I bond of proteins, ester, or ether; and C–N of aliphatic amines or alcohol/phenol, respectively (Ibrahim 2015; Velmurugan et al.

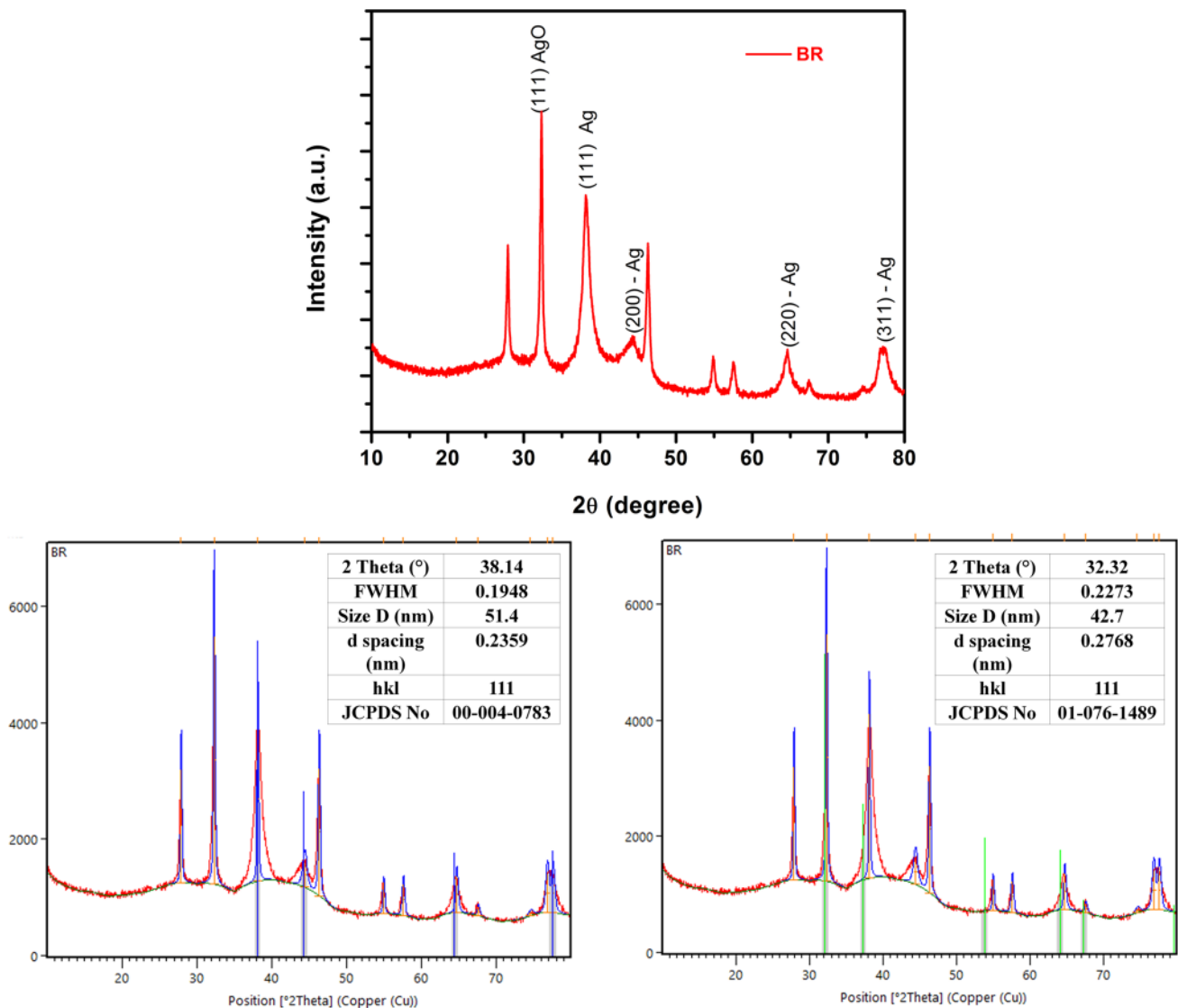


Fig. 5 X-ray diffraction patterns of synthesized Ag₂O NPs

2016). The obtained AgNPs show a shift in the peaks at 3360, 2922, 1631, 1383, and 1058/cm, corresponding to the hydroxyl and amide groups on the surface of the FBPRES, which could be responsible for the reduction of Ag⁺. FBPRES mainly contains flavonoids, saponins, steroids, reducing sugars, alkaloids, antimony trioxide, tannins, glycosides, antimony trisulfide, 1,2-dihexanoyl-sn-glycero-3-phosphocholine, α -ethyl- α -phenyl glutarimide, 2,2,2-trichloroethanol, and 2-chloroethyl phosphonic acid, which was previously reported by Kumar et al. (2010), and might be involved in reducing the Ag⁺ to Ag⁰.

HR-TEM

The HR-TEM image showed a more spherical shape and monodispersed Ag₂O NPS with an average particle size of ~10 to 60 nm (Fig. 4). The particle size distribution graph shows that the mean diameter of silver oxide 42.7 nm and silver 51.4 nm (Fig. 4). The crystalline nature of the Ag₂O NPS was confirmed based on the bright circular spots obtained in SAED patterns (Fig. 4).

XRD

The powder X-ray diffraction spectra of the formed Ag₂O NPs were displayed in (Fig. 5), confirming the occurrence of genuine Ag₂O NPS. The XRD spectra obtained were confirmed against the standard spectra of Ag₂O (JCPDS no. 00-012-0793). At 2 θ values of 32.06°, 40.03°, 65.03°, and 79.84°, several Bragg reflection peaks were observed, which are indexed to (111), (200), (220), and (311) planes of pure

Ag₂O NPs, respectively, matching those of the standard spectra of silver (JCPDS no.# 00-004-0783) with a 51.4 nm and silver oxide (JCPDS no.# 01-076-1489) with 42.7 nm.

XRD analysis, therefore, confirms the face-centered cubic (FCC) configuration of biosynthesized Ag₂O NPs using software PANalytical X'Pert High Score Plus, Version 3.0.3 (Fig. 5). According to Scherrer equation, the mean particle diameter of the Ag₂O NPs was calculated from the XRD pattern:

$$D = K\lambda/\beta_{1/2}\cos\theta.$$

The shape constant is K , wavelength of the X-ray is λ , and $\beta_{1/2}$ and θ are the half width of the peak and half of the Bragg's angle, respectively. The calculated average crystallite size of the Ag₂O NPs was found to be between 14.6 and 32.6 nm from the breadth of the (111) reflection.

Antibacterial activity

The antibacterial efficiency of the FBPRES, FBPRES + Ag₂O NPS, Ag₂O NPS, Ag⁺, and commercial Ag NPs against dental bacteria was tested against *S. mutans* and *L. acidophilus* by ZOI and MBC with appropriate controls. The inhibition zones yielded by the various materials are shown in (Table 1). The data showed that the synthesized Ag₂O NPS, FBPRES, FBPRES + Ag₂O NPS, Ag⁺, and commercial Ag NPs each showed different levels of antibacterial activity by indicator organisms. The blend of FBPRES + Ag₂O NPS shows maximum inhibition zones of 15 and 18 mm against *S. mutans* and *L. acidophilus* at higher concentrations of 250 μ g, respectively. These

Table 1 Antibacterial activity (ZOI, and MBC) of FBPRES, FBPRES +Ag₂O NPS, Ag₂O NPS, Ag⁺, Commercial Ag NPs penicillium control against dental bacteria

Bacterial strains	ZOI (mm)					MBC (%)				
	<i>S. mutans</i>					<i>L. acidophilus</i>				
Concentration (μ g)	50	100	150	200	250	50	100	150	200	250
FBPRES	–	–	3 \pm 0.2	5 \pm 0.2	6 \pm 0.8	–	–	6 \pm 0.6	7 \pm 0.3	7 \pm 0.9
FBPRES +Ag ₂ O NPS	–	6 \pm 0.4	10 \pm 0.9	13 \pm 0.2	15 \pm 0.7	–	–	20 \pm 0.4	24 \pm 0.8	29 \pm 0.1
Ag ₂ O NPS	–	–	3 \pm 0.5	5 \pm 0.2	6 \pm 0.8	–	–	12 \pm 0.2	18 \pm 0.4	22 \pm 0.2
Ag ⁺	–	3 \pm 0.4	5 \pm 0.8	7 \pm 0.7	8 \pm 0.2	3 \pm 0.4	8 \pm 0.5	12 \pm 0.8	16 \pm 0.6	20 \pm 0.2
Commercial Ag NPs	2 \pm 0.9	5 \pm 0.5	7 \pm 0.5	9 \pm 0.4	12 \pm 0.1	6 \pm 0.8	9 \pm 0.2	13 \pm 0.4	15 \pm 0.8	18 \pm 0.5
Penicillium control*	20 \pm 0.7	23 \pm 0.4	26 \pm 0.5	32 \pm 0.6	38 \pm 0.5	42 \pm 0.8	65 \pm 0.7	73 \pm 0.6	86 \pm 0.7	98 \pm 0.6
FBPRES	–	–	5 \pm 0.7	7 \pm 0.4	8 \pm 0.1	–	–	6 \pm 0.5	8 \pm 0.7	10 \pm 0.5
FBPRES +Ag ₂ O NPS	–	8 \pm 0.7	13 \pm 0.7	15 \pm 0.8	18 \pm 0.6	–	–	23 \pm 0.7	27 \pm 0.7	30 \pm 0.4
Ag ₂ O NPS	–	–	3 \pm 0.5	6 \pm 0.5	8 \pm 0.4	–	–	15 \pm 0.9	19 \pm 0.2	25 \pm 0.5
Ag ⁺	–	4 \pm 0.8	5 \pm 0.2	7 \pm 0.5	8 \pm 0.2	3 \pm 0.4	5 \pm 0.9	14 \pm 0.9	16 \pm 0.8	21 \pm 0.7
Commercial Ag NPs	2 \pm 0.7	7 \pm 0.8	7 \pm 0.4	9 \pm 0.9	12 \pm 0.5	8 \pm 0.6	13 \pm 0.4	15 \pm 0.5	18 \pm 0.7	20 \pm 0.5
Penicillium control*	22 \pm 0.4	26 \pm 0.2	28 \pm 0.6	34 \pm 0.7	40 \pm 0.5	32 \pm 0.7	45 \pm 0.3	63 \pm 0.7	76 \pm 0.2	96 \pm 0.5

* Concentrations 1, 2, 4, 8 and 16 μ g/mL

represented the largest inhibition zones and were followed in terms of efficiency by commercial AgNPs and Ag⁺ ions. Additionally, the Ag₂O NPs, FBPRES, and Ag⁺ show moderate inhibition zones against *S. mutans* and *L. acidophilus* at a higher concentration of 250 µg. The percentages of MBC for synthesized Ag₂O NPS, FBPRES, FBPRES + Ag₂O NPS, Ag⁺, and commercial AgNPs are shown in (Table 1). The blend of synthesized Ag₂O NPS and FBPRES showed a remarkable percentage of bactericidal activity against *S. mutans* and *L. acidophilus*, followed by those of Ag₂O NPS, commercial AgNPs, FBPRES, and Ag⁺ at a higher concentration of 250 µg.

Conclusion

Ficus benghalensis prop root extract as an easily available substrate and no cost material was successfully utilized for the reliable and rapid synthesis of Ag₂O NPS. The photo-synthesized Ag₂O NPS using FBPRES were examined for their physical characters, and they were found to be crystalline, uniform, spherical, and monodispersed nanoparticles with an average particle size of silver oxide 42.7 nm and silver 51.4 nm. The blend of synthesized Ag₂O NPs and FBPRES revealed good antimicrobial activity against the selected dental bacterial strains. This green synthesis approach enables a new avenue to produce Ag₂O NPS as an eco-friendly alternative with non-toxic as a safe mode alternative to physical and chemical methods, and would be suitable for process for large-scale production. The overall study suggests that a blend of synthesized Ag₂O NPS and FBPRES will be useful in tooth paste as a germicidal agent after extensive investigation with animal models.

Acknowledgements This work was supported by the BK21 plus program through the National Research Foundation (NRF) funded by the Ministry of Education of Korea. This work was also supported by the National Research Foundation of Korea (NRF) funded by the Ministry of Science, ICT and Future Planning (NRF-2016R1C1B2009865).

Compliance with ethical standards

Conflict of interest The author(s) declare(s) that there is no conflict of interest regarding the publication of this paper.

References

- Ahmad S, Rao H, Akhtar M, Ahmad I, Hayat MM, Iqbal Z (2011) Phytochemical composition and pharmacological prospectus of *Ficus benghalensis* Linn. (Moraceae)-A review. *J Med Plants Res* 5:6393–6400
- Ahmed S, Ahmad M, Swami BL, Ikram S (2016) Green synthesis of silver nanoparticles using *Azadirachta indica* aqueous leaf extract. *J Radiat Res Appl Sci* 9:1–7
- Amin M, Anwar F, Janjua MR, Iqbal MA, Rashid U (2012) Green synthesis of silver nanoparticles through reduction with *Solanum xanthocarpum* L. berry extract: characterization, antimicrobial and urease inhibitory activities against *Helicobacter pylori*. *Int J Mol Sci* 13:9923–9941
- Aswar M, Aswar U, Watkar B, Vyas M, Wagh A, Gujar K (2008) Anthelmintic activity of *Ficus benghalensis*. *Int J Green Pharm* 2:170–172
- Chitra K, Annadurai G (2014) Antibacterial activity of pH-dependent biosynthesized silver nanoparticles against clinical pathogen. *Biomed Res Int*. doi:10.1155/2014/725165
- Dong C, Cao C, Zhang X, Zhan Y, Wang X, Yang X, Zhou K, Xiao X, Yuan B (2017) Wolfberry fruit (*Lycium barbarum*) extract mediated novel route for the green synthesis of silver nanoparticles. *Optik* 130:162–170
- Dwivedi AD, Gopal K (2010) Biosynthesis of silver and gold nanoparticles using *Chenopodium album* leaf extract. *Colloids Surf A* 369:27–33
- Ibrahim HM (2015) Green synthesis and characterization of silver nanoparticles using banana peel extract and their antimicrobial activity against representative microorganisms. *J Radiat Res Appl Sci* 8:265–275
- Kora AJ, Sashidhar RB, Arunachalam J (2010) Gum kondagogu (*Cochlospermum gossypium*): a template for the green synthesis and stabilization of silver nanoparticles with antibacterial application. *Carbohydr Polym* 82:670–679
- Kumar G, Karthik L, Bhaskara Rao KV (2010) Antimicrobial activity of latex of *Calotropis gigantea* against pathogenic microorganisms-an in vitro study. *Pharmacologyonline* 3:155–163
- Lee HJ, Song JY, Kim BS (2013) Biological synthesis of copper nanoparticles using *Magnolia kobus* leaf extract and their antibacterial activity. *J Chem Technol Biotechnol* 88:1971–1977
- Loesche WJ (1986) Role of *Streptococcus mutans* in human dental decay. *Microbiol Rev* 50:353–380
- Marcotte H, Lavoie MC (1998) Oral microbial ecology and the role of salivary immunoglobulin A. *Microbiol Mol Biol Rev* 62:71–109
- Marsh PD (2010) Microbiology of dental plaque biofilms and their role in oral health and caries. *Dent Clin North Am* 54:441–454
- Muthukrishnan S, Bhakya S, Kumar TS, Rao MV (2015) Biosynthesis, characterization and antibacterial effect of plant-mediated silver nanoparticles using *Ceropegia thwaitesii*-an endemic species. *Ind Crops Prod* 63:119–124
- Nidhiya IS, Pai KS, Rao MC (2010) Free radical scavenging activity of extracts of young prop roots of *Ficus benghalensis*. *Pharmacologyonline* 2:299–307
- Okafor F, Janen A, Kukhtareva T, Edwards V, Curley M (2013) Green synthesis of silver nanoparticles, their characterization, application and antibacterial activity. *Int J Environ Res Publ Health* 10:5221–5238
- Palanisamy S, Rajasekar P, Vijayaprasath G, Ravi G, Manikandan R, Prabhu NM (2017) A green route to synthesis silver nanoparticles using *Sargassum polycystum* and its antioxidant and cytotoxic effects: an in vitro analysis. *Mater Lett* 189:196–200
- Panday DR, Rauniar GP (2016) Effect of root-extracts of *Ficus benghalensis* (Banyan) in memory, anxiety, muscle co-ordination and seizure in animal models. *BMC Complement Altern Med* 16:429–441
- Pourmortazavi SM, Taghdiri M, Makari V, Rahimi-Nasrabadi M (2015) Procedure optimization for green synthesis of silver nanoparticles by aqueous extract of *Eucalyptus oleosa*. *Spectrochim Acta Mol Biomol Spectrosc* 136:1249–1254
- Raut Rajesh W, Lakkakula Jaya R, Kolekar Niranjan S, Mendhulkar Vijay D, Kashid Sahebrao B (2009) Phytosynthesis of silver nanoparticle using *Gliricidia sepium* (Jacq.). *Curr Nanosci* 5:117–122



- Shankar SS, Rai A, Ahmad A, Sastry M (2004) Rapid synthesis of Au, Ag, and bimetallic Au core–Ag shell nanoparticles using Neem (*Azadirachta indica*) leaf broth. *J Colloid Interface Sci* 275:496–502
- Vanaja M, Rajeshkumar S, Paulkumar K, Gnanajobitha G, Malarkodi C, Annadurai G (2013) Phytosynthesis and characterization of silver nanoparticles using stem extract of *Coleus aromaticus*. *Int J Mater Biomater Appl* 3:1–4
- Velmurugan P, Lee SM, Cho M, Park JH, Seo SK, Myung H, Bang KS, Oh BT (2014) Antibacterial activity of silver nanoparticle-coated fabric and leather against odor and skin infection causing bacteria. *Appl Microbiol Biotechnol* 98:8179–8189
- Velmurugan P, Sivakumar S, Song YC, Jang SH (2015) Crystallization of silver metal by extract of *Prunus × yedoensis* Matsumura blossoms and its potential characterization. *J Ind Eng Chem* 31:39–42
- Velmurugan P, Shim J, Bang KS, Oh BT (2016) Gold nanoparticles mediated coloring of fabrics and leather for antibacterial activity. *J Photochem Photobiol B* 160:102–109
- Verma A, Mehata MS (2016) Controllable synthesis of silver nanoparticles using Neem leaves and their antimicrobial activity. *J Radiat Res Appl Sci* 9:109–115